Ordered Structure in Blends of Block Copolymers. 4. Location of the Short Diblock†

Daisuke Yamaguchi,‡ Jeffrey Bodycomb,‡,§ Satoshi Koizumi,|| and Takeji Hashimoto*,‡

Department of Polymer Chemistry, Graduate School of Engineering, Kyoto University, Kyoto 606-8501, Japan, and Advanced Science Research Center, Japan Atomic Energy Research Institute, Tokai, Ibaraki 319-1112, Japan

Received April 8, 1999; Revised Manuscript Received June 29, 1999

ABSTRACT: We used small-angle neutron scattering (SANS) and small-angle X-ray scattering (SAXS) to examine a blend of two polystyrene-*block*-polyisoprene polymers with different molecular weights (6.73×10^4 and 1.0×10^4) and volume fractions of polystyrene (0.81 and 0.52, respectively), i.e., a blend of the type $(A-B)_\alpha/(A-B)_\beta$. The results show that the junctions of the short diblock copolymer are localized at the interface in the lamellar microdomains at low temperatures with a relatively strong segregation and that more of the short diblock copolymer is delocalized with their junctions moving away from the interface with increasing temperature. The domain spacing is seen to decrease with the addition of the short diblock to the long diblock copolymer at a given temperature. The domain spacing of blends with a large amount of the short diblock is seen to increase or stay constant with increasing temperature, which is radically different from the behavior of pure diblock copolymers or their blends with homopolymer. The SANS results indicate that the first-order scattering peak is of a much lower intensity than expected, compared with the SAXS results, or in some cases suppressed completely. For the case of the 60/40 (w/w) blend, the first-order peak is suppressed at low temperatures and appears at high temperatures, indicating delocalization of the short diblock. All of these results are consistent with the picture that the junction of the short diblock is localized at the interface but the degree of localization decreases with increasing temperature.

I. Introduction

Diblock copolymers and their blends have received much experimental and theoretical attention due to their interesting and potentially useful properties, among which is the formation of a microphase-separated system.[1,2] Blends of diblock copolymers with other, chemically similar diblock copolymers have received some attention,[3−9] but little compared to studies on blends of diblock copolymers and homopolymers.[10] Recently, there has been some theoretical work done on these systems[11−13] because of the interesting phase behavior of these materials.[3−8]

Binary blends of diblock copolymers of the type A−B/A−B have been shown to have a broad array of interesting behavior, including macrophase separation,[5] microphase separation,[3,4] macrophase separation induced by microphase separation,[6,7] order−order transitions,[8,9] and modulated or superlattice structures.[7]

Shi and Noolandi have presented theoretical calculations and show that the location of the short diblock in the microdomain space is a function of the composition of the short diblock. The location of the short diblock chains varies from being localized with their junctions between the two block chains at the interface for the case where the block copolymer is symmetric to the case where it is dissolved into one microphase or the other for the case where the composition of the short diblock is highly asymmetric.[11] As the location of the short diblock changes, the resulting structure of the blend of diblock copolymers also changes. Furthermore, Lin et al. used small-angle X-ray scattering (SAXS) to examine the effect of short diblock on the domain spacing of a blend of diblock copolymers and showed that the short diblock is localized at the interface.[14]

Other recent work on block copolymer/block copolymer blends of the type A−B/A−B by Sakurai et al.[15] shows that the dependence of the domain spacing of these blends as a function of temperature can be the opposite of that seen in pure diblock copolymers. That is, in pure diblock copolymers and their blends with homopolymers, the domain spacing decreases with increasing temperature, while in the case of a blend of the type A−B/A−B, the opposite behavior is observed.

Small-angle neutron-scattering techniques have been successfully used to identify chain conformation of one block in pure diblock copolymer systems[16−20] and the distribution of homopolymer in diblock copolymer/homopolymer blends[21−24] by taking advantage of a difference in contrast between deuterium labeled polystyrene and the usual protonated polystyrene. For block copolymer/block copolymer blends of the type A−B/A−B, Mayes et al. examined mixtures of high and low molecular weight polystyrene-*block*-poly(methyl methacrylate) copolymers in spin-coated thin films by using the neutron reflectivity method.[25] From the reflectivity experiments on mixtures which contain the deuterium labeled block as one component, they determined the spatial distributions of the high and low molecular weight copolymer blocks.[25]

In this study, we use the difference in contrast between deuterated and protonated polystyrene to identify the location of one component of a blend in the microdomain space developed by the mixtures. In this

* To whom correspondence should be addressed.

† Presented in part at the 45th Symposium of the Society of Polymer Science, Japan, Oct, 1996. *Polym. Prepr. Jpn., Soc. Polym. Sci., Jpn.* **1996**, *45*, 2179−2180.

‡ Kyoto University.

§ Present address: Polymer Dynamics, PO Box 4400, 2200 South 12th Street, Allentown, PA 18103.

|| Japan Atomic Energy Research Institute.

10.1021/ma990534o CCC: $18.00
Published on Web 08/07/1999

work, we will examine the effect of both temperature and blend composition on the location of the short diblock. It is expected that these results will assist in understanding the origin of the behavior of these materials as a function of temperature and composition.

We chose a blend system that did not show any order−order transitions over the temperature range studied. While such order−order transitions are among the more interesting behaviors observed in block copolymer systems, they also complicate interpretation considerably. Furthermore, we examine the relatively simple case of a lamellar system, which we can readily model. Even for this case, due to the deuterium labeling effect, we observe unusual scattering behavior from this system that strongly suggests that the junction of the short diblock copolymer at the interface leaves the interface with increasing temperature and the short diblock swells one of the domains or both domains, leading to unusual changes in domain spacing with changes in temperature.

II. Experimental Section

Diblock copolymers, polystyrene-*block*-polyisoprene (SI), were synthesized by living anionic polymerization with *sec*-butyllithium as an initiator and cyclohexane as a solvent. The polymer molecular weight was characterized by GPC. The polymer characteristics are designated according to the scheme presented by Winey et al.[26] Two SI diblock copolymers were used in this study, the long one of which, designated SI-56-12, has a number-average molecular weight M_n of 5.56×10^4 for the protonated polystyrene (hPS) block and $M_n = 1.17 \times 10^4$ for the polyisoprene (PI) block. The short diblock, designated dSI-5−4 is a short diblock with a deuterated PS (dPS) block having $M_n = 5.5 \times 10^3$ and a (protonated) PI block having $M_n = 4.5 \times 10^3$. In both cases the polydispersity index, M_w/M_n, was less than 1.05. Film specimens were cast from a 5 wt % polymer in toluene solution. After casting, orientation of the lamellae existing in the cast films was randomized by mechanical agitation at a temperature above the glass transition temperature of the PS (>100 °C). Three blends were prepared with different compositions and are designated 80/20, 70/30, and 60/40 to denote the weight ratio of the long diblock to the short diblock.

Temperature-dependent small-angle X-ray-scattering, SAXS, was measured in situ with a SAXS apparatus described elsewhere, except, in some cases, for the replacement of the X-ray generator with a new one (MAC Sciences M18X HF operated at 18 kW).[27−29] All measurements were conducted with specimens placed in an evacuated chamber to reduce thermal degradation. SAXS profiles were desmeared for slit-width and slit-height smearing and corrected for air scattering, absorption, and thermal diffuse scattering.[27−29]

The small-angle neutron-scattering (SANS) experiments were performed with a 20 m SANS instrument (SANS-J) at the JRR-3M research reactor at the Japan Atomic Energy Research Institute (JAERI) in Tokai, Japan. Data were collected with a two-dimensional Risø-type detector and corrected for scattering from the empty cell, detector sensitivity, and absorption by the sample. The sample to detector distance was 4 m for the 80/20 and 60/40 blends and 5 m for the 70/30 blend. The electrical background of this instrument is small enough to be neglected over the q range covered in this work where q is the magnitude of the scattering vector $q = (4\pi/\lambda)\sin(\theta/2)$ with λ and θ being wavelength and scattering angle of incident radiation. The two-dimensional data were circularly averaged to obtain scattering profiles as a function of q. The experiments were conducted by cooling the sample in steps and allowing the sample to anneal 1 h between measurements. The neutron-scattering experiments were conducted on two different occasions, and therefore, the weighting functions for the SANS optics differ. While smearing effects are substantial, they do not modify the conclusions of this work.

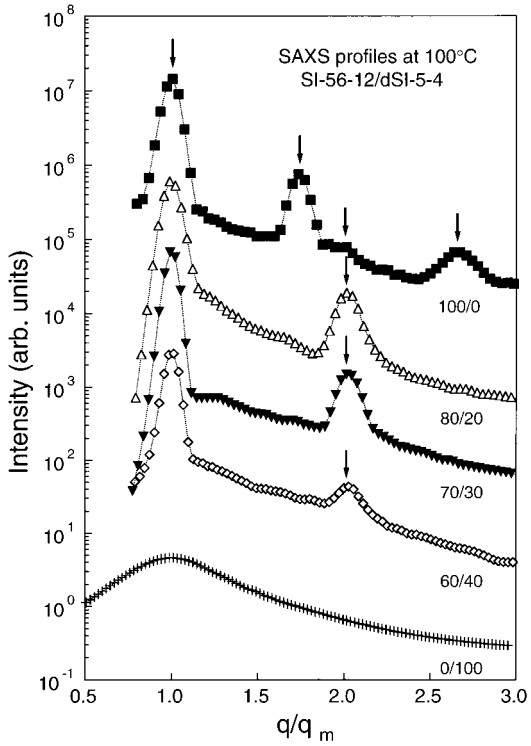

Figure 1. SAXS profiles of various blends at 100° C to display the different morphologies. Successive curves were shifted down by one decade each for clarity. Key: (■) pure SI-56-12; (△) 80/20 blend; (▼) 70/30 blend; (◇) 60/40 blend; (+) pure dSI-5-4.

III. Results

A. SAXS Results. In Figure 1, we show the desmeared SAXS profiles of each of the blends as well as the two pure diblock copolymers at 100 °C where q is scaled with q_m, the q value at the first-order scattering maximum. In all cases except that of the short diblock copolymer, dSI-5-4, we observe scattering profiles from which we could identify at least the first two peaks. Thus, we can determine the structure of these materials from the SAXS data. For the pure long diblock (SI-56-12), we observe scattering peaks with q values having a ratio of $1:\sqrt{3}:\sqrt{4}:\sqrt{7}$, which are indicative of a hexagonally packed cylindrical morphology, as expected from a volume fraction of 0.81 for PS.[30] The short diblock copolymer only shows a single broad scattering peak indicative of a disordered system. Since this block copolymer has such a low molecular weight, the ODT is below the glass transition of the PS block and is therefore inaccessible.[1,31,32] Unlike either of the pure diblock copolymers, the three blends examined here show SAXS peaks with q values having a ratio of 1:2, which is indicative of lamellar structure.

In Figure 2, we show the desmeared SAXS patterns at various temperatures for the three blends discussed here. On each figure, the insets show the change in the second-order peak height (left axis of the inset), $I_m/I_{m,100}$, and position (right axis of the inset), $q_m/q_{m,100}$, scaled with the peak height and position at 100 °C, respectively as a function of temperature.

Figure 2a shows the SAXS patterns from the 80/20 blend. At 180 °C the first-order peak is clearly discerned, while the second-order peak is very weak. As temperature is decreased to 140 °C the first-order peak becomes slightly more intense while the second-order peak becomes substantially more intense. Furthermore,

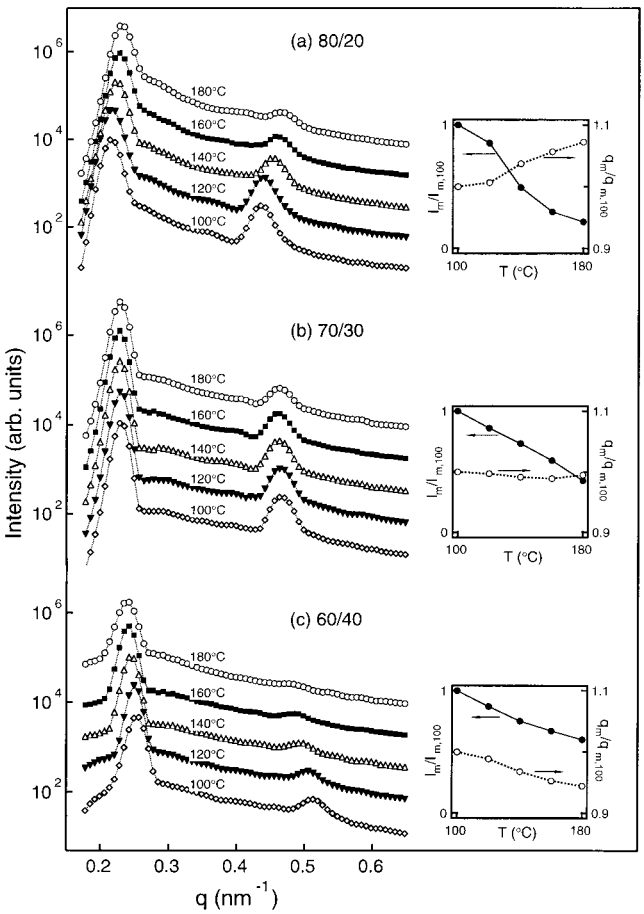

Figure 2. SAXS profiles of blends at various temperatures: (a) 80/20 blend, (b) 70/30 blend, and (c) 60/40 blend. Key: (○) 180 °C; (■) 160 °C; (△) 140 °C; (▼) 120 °C; (◇) 100 °C. Insets show the peak height (left axis, ● and solid line) and position (right axis, ○ and dashed line) of the second-order peak scaled with the peak height and position at 100 °C, respectively.

both peak positions shift to the left (lower q value), indicating an increase in domain spacing with cooling for this sample. Finally on cooling to 100 °C, this trend continues with further small increases in the height of the first-order peak and large increases in the second-order peak height along with an increase in lamellar spacing.

Figure 2b shows SAXS patterns from the 70/30 blend. Here, at 180 °C the second-order peak is more clear compared with the 80/20 blend. Similar to the 80/20 blend, as the temperature is decreased to 140 °C the second-order peak height increases dramatically, while the first-order peak height does not increase as much. However, the peak positions do not change, indicating no change in domain spacing with decreasing temperature but a change in relative thickness of PS and PI lamella. On further cooling to 100 °C, the second-order peak further increases in intensity and the lamellar spacing remains constant.

Figure 2c shows the SAXS patterns from the 60/40 blend at five temperatures as well. Similar to that for the 80/20 blend, the second-order peak is very weak at 180 °C. As temperature is lowered to 140 °C the second-order peak grows dramatically, similar to what is observed for the other two blends. However, the peak positions shift to the right (increasing q values), indicating that with decreasing temperature the domain spacing is decreasing, opposite the behavior that is usually

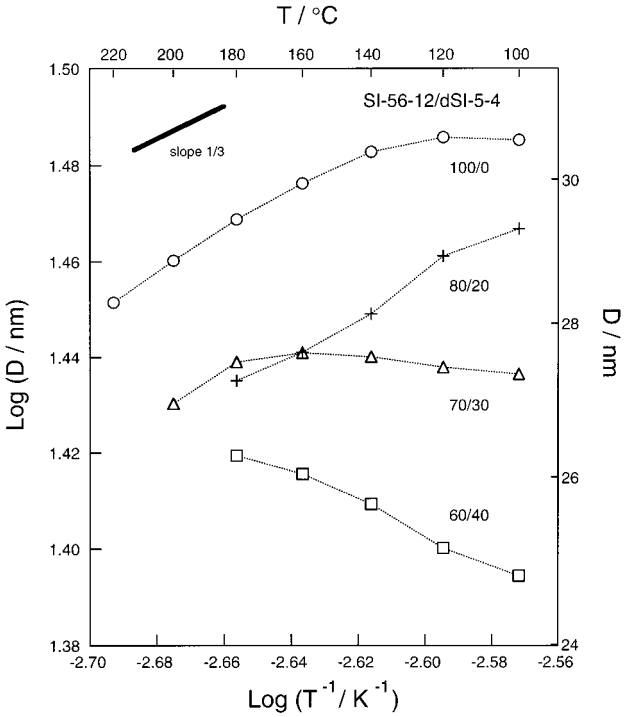

Figure 3. Plot of log D vs log $1/T$ as measured by SAXS. Key: (○) pure SI-56-12; (+) 80/20 blend; (△) 70/30 blend; (□) 60/40.

observed in block copolymers and in the 80/20 blend (Figure 2c). When the temperature is further lowered to 100 °C, the first- and second-order peak heights increase while the peak position continues to shift to the right; that is, lamellar spacing is decreasing.

In all three blends shown here, particularly at lower temperatures, the first-order and second-order peaks are readily discerned. Furthermore, there is no upturn in the SAXS patterns at low q, which indicates no macrophase separation. As the temperature is decreased, both the first- and second-order peaks become stronger. However, the second-order peak becomes stronger more quickly. Furthermore, the relative peak positions of the first-order and the second-order peaks do not change with temperature, indicating that these blends do not show an order−order transition (OOT) and hence keep the lamellar morphology in the temperature range studied. The SAXS behavior described above here is typical of most diblock copolymer systems. That is, the peak height increases with decreasing temperature. However, when one examines the position of the first-order scattering peak in order to evaluate the domain spacing, the results are unusual.

To quantitatively identify the peak positions and heights, SAXS peaks were fit with a Gaussian function. From the fitting parameters, we obtained the maximum scattered intensity I_m and position of each peak q_m. From the value of q_m for the first-order peak, we can identify the domain spacing, $D = 2\pi/q_m$. From these fits, we obtain domain spacing for each blend sample as a function of temperature, which is shown in Figure 3. The behavior of the pure long diblock is typical of that reported earlier.[33] That is, with increasing temperature, the domain spacing decreases. On the addition of short diblock, at a constant temperature, the domain spacing is seen to decrease. However, the effect of temperature on the domain spacing of a particular blend depends on the volume fraction of the short diblock in the system.

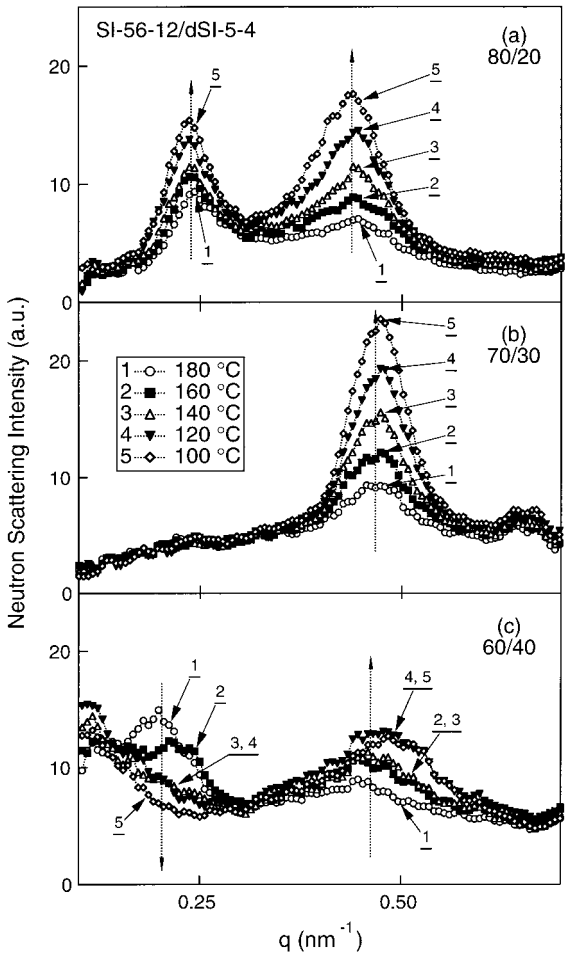

Figure 4. SANS profiles at various temperatures: (a) 80/20 blend, (b) 70/30 blend, and (c) 60/40 blend. Key: (○) 180 °C; (■) 160 °C; (△) 140 °C; (▼) 120 °C; (◇) 100 °C.

We see that, for the pure diblock and 80/20 blend, the domain spacing increases with decreasing temperature, which is consistent with other studies on SI diblock systems. However, on the further addition of the short diblock, the domain spacing becomes nearly temperature independent for the 70/30 blend, and finally for the 60/40 blend, it increases with increasing temperature, which is the reverse of what is typically expected. As we increase the amount of the short diblock in the blend, the reverse temperature dependence of the domain spacing becomes more important, thus suggesting that the short diblock is responsible for this behavior.

B. SANS Results. Further insight into the behavior of these samples can be obtained by neutron-scattering measurements since one polymer in the blend has a dPS block and the other block copolymer has an hPS block. A typical SANS measurement with a two-dimensional detector gave the nearly circular rings pattern with respect to the incident beam axis. This indicates that the lamellae in the blend sample have macroscopically random orientation. The scattering rings corresponding to the first- and/or second-order scattering peaks from the lamellar microdomains of an isotropic polymer sample. Since the sample is isotropic, in subsequent discussion we use circularly averaged scattering data, shown as a function of the magnitude of the scattering vector **q** in Figure 4.

The SANS behavior shown in Figure 4 is dramatically different from what one would expect after examining the SAXS data. Figure 4 shows the circularly averaged scattering data for each blend at different temperatures. The arrows indicate the change in peak heights with decreasing temperature. A plot of the changes in peak heights with temperature is given later in Figure 8.

For the case of the 80/20 blend, shown in Figure 4a, the first-order peak is somewhat stronger than the second-order peak at 180 °C. Note, however, that the difference in peak heights is small compared to that observed in the SAXS data shown in Figure 2. As the temperature is decreased, the height of the second-order peak increases more quickly than the height of the first-order peak. At 120 °C (curve 4) the second-order peak is nearly the same magnitude as the first-order peak. Finally, at 100 °C (curve 5), the second-order peak is somewhat stronger than the first-order peak. This is very unusual compared to the X-ray scattering data showing that the first-order peak height was an order of magnitude larger than the second-order peak height (Figure 2a). However, similar to the X-ray scattering data, the peak heights did increase with decreasing temperature. It is worthwhile noting that in the neutron reflectivity experiment, as well,[25] some mixtures of high and low molecular weight polystyrene-*block*-poly(methyl methacrylate) copolymers in which one of the blocks in the low molecular weight block copolymer is deuterium-labeled show the reflectivity profiles with a very large second-order maximum compared with the first-order maximum. The corresponding model scattering length density profiles indicate that there is an excess of deuterated blocks at the microdomain interfaces, implying a localization of the low molecular weight component to the interfacial region.[25]

The 70/30 blend shown in Figure 4b has no first-order peak at all at any temperature. However, from the SAXS measurements, we certainly expect one at about $q \approx 0.23$ nm^{-1}. The second-order peak, which occurs at nearly the same q value as the second-order peak in the SAXS measurement, shows typical behavior in that it becomes stronger with decreasing temperature, as indicated by the arrows showing the tendency.

Finally, the 60/40 blend sample does not seem to have a first-order peak[34] at 100 °C (curve 5), but with increasing temperature, the first-order scattering peak appears and its intensity increases. Namely, for this blend, the intensity decreases with decreasing temperature, which is just opposite of what we observe in the SAXS measurement where the first-order peak decreases with increasing temperature (see Figure 2). In contrast to this unusual temperature dependence of the first-order scattering peak, the second-order scattering peak shows more typical behavior in that it increases with decreasing temperature.

In summary, for this series of blends, by SAXS we observe that the effect of temperature on domain spacing is unusual, while the effect of temperature on the peak intensities is typical of block copolymer systems. Furthermore, by SANS, we observe that the effect of temperature on the peak heights and positions is very unusual.

IV. Discussion

From the SAXS data, we observe that on addition of the short block copolymer, the domain spacing of the blend decreases (Figure 3). This effect is because we are effectively increasing the interface area per unit volume by increasing the number of junctions per unit volume

by adding the short diblock copolymer. The structural transition on the addition of the short diblock has been reported previously[5,8,14] and is presumed to arise due to the combined effect of changing the volume fraction of PS in the system and the effect of the short diblock at the interface changing the curvature of the interface (the cosurfactant effect). Here, we are interested in the change in domain spacing as a function of temperature.

Let us begin by considering the pure block copolymer case. Here, the domain spacing decreases with increasing temperature due to the fact that as the temperature increases, the net repulsive interactions between the PS and PI weaken,[33] allowing a larger interfacial area per unit volume.

However, we observe that the domain spacing of the blends shows an unusual temperature dependence. This behavior has been reported previously for a similar type of blend.[15] We postulate that as temperature is raised, the short block copolymer preferentially dissolves into one or both of the lamellae. Therefore, the effective interface area per unit volume is decreased, leading to a larger domain spacing. This is slightly different from the model proposed by Sakurai et al.[15] In their description, as the temperature increases, the miscibility between the PS and PI block chains increases, and therefore the shorter chains become closer and cause the interface to undulate. As the interface undulates, the long chains stretch to prevent chain overlap, leading to a larger domain spacing. However, here we consider that the interface remains straight as the short block dissolves into one microphase of the microphase-separated system, removing the short diblock junctions from the interface and, therefore, decreasing the interfacial area per unit volume at higher temperatures, increasing the domain spacing. Moreover we confirm the validity of this postulate or model by the use of SANS and the deuterium labeling effect as will be discussed below.

In the case of a blend of two block copolymers, in addition to considering the interactions between blocks, as in the case of pure block copolymer, one must also consider the effect of temperature on the solubility of one polymer in each microphase. As temperature is increased, for a system showing UCST behavior, the short diblock will be more soluble in either block of the long block copolymer; that is, it will be more soluble in either microphase. At higher temperatures, the short block copolymer is presumed to leave the interface by dissolving into one or both of the microphases of the phase-separated polymer, thus decreasing the interface area per unit volume and therefore increasing the domain spacing with increasing temperature. For the 80/20 blend, the effect of the short diblock leaving the interface is presumably too weak to affect the domain spacing. However, for the 70/30 blend this effect counter balances the tendency for domain spacing to decrease with increasing temperature, giving a temperature-independent domain spacing. Finally, for the 60/40 blend, this effect is dominant over the other effect, as we observe that the usual temperature-dependent behavior is reversed. From these data, we postulate that the short diblock leaves the interface with increasing temperature and swells one phase and/or both phases of the lamella. Once the short diblock has left the interface, the interfacial surface area per unit volume should decrease leading to an increase in domain spacing. Below, we will discuss how the SANS results are consistent with this hypothesis.

By using the labeled short diblock, we have obtained surprising, counterintuitive neutron-scattering results when the data are considered both when a single temperature is studied and when the effect of temperature is considered. These effects can be explained if one considers the deuterium-labeling effect. Due to the fact that the polystyrene block of the short diblock is deuterated and the tendency of the short diblocks to exist with their junctions at the interface, an unusual scattering length profile is present, which leads to unusual scattering behavior.

To explain this behavior, we begin with a simple model that captures the features of the system under study. We can regard lamellae at low temperature as having a spatial distribution of short and long diblock as shown in Figure 5a where the junctions of the long and short diblocks are localized at the interface and each block segregates properly into each domain. It will then have the spatial distribution of scattering length density for SANS shown in Figure 5b, and, finally, an electron density profile for SAXS shown in Figure 5c.

As the temperature is increased, the short block copolymer will dissolve into one of the lamellar phases or both lamellar phases. A schematic of the process at higher temperature is depicted in Figure 5d, and the resulting scattering length profile and electron density profile are shown in parts e and f of Figure 5, respectively. Parts d−f of Figure 5 assume a uniform distribution of dSI in the domain space for simplicity. As the short diblock dissolves into one of the lamellar domains, the domain spacing increases such that the spacing in 5d−f is greater than the spacing in Figure 5a−c. This increase in D can be readily imagined if one considers that as the short diblock dissolves into one lamellar domain, its junction is no longer contributing to the interfacial area. Thus, the interfacial area per unit volume decreases, and hence D increases. This change is observable by both SAXS and SANS as a change in domain spacing. The change in contrast in a SANS measurement (from Figure 5b to Figure 5e) is much more dramatic than that in a SAXS measurement (from Figure 5c to Figure 5f), due to the big contrast difference between dPS and hPS for SANS experiments.

The scattering amplitude for the model in Figure 5b with the **q** vector in the direction normal to the interface, $f(q)$, is given as

$$f(q) \propto \left\{ \frac{I_d \sin(qD_s/2) - (l_d - l_s) \sin[q(D_s - 2D_d)/2]}{q/2} \right\} \quad (1)$$

where l_d is the scattering length of the dPS rich region in the PS lamellae minus that of the PI lamellae, l_s is the scattering length of the hPS region minus that of the PI region. D_s is the width of the PS lamellae, D_d is the width of the deuterium-rich region in the PS lamellae, and D is the domain spacing. These dimensions are shown in Figure 5b. For SAXS experiments, l_d and l_s in eq 1 are equivalent and read as electron densities. In the case of model d for the uniform distribution of the short diblock, l_d and l_s in eq 1 are again equivalent for both SANS and SAXS: l_d is the average scattering length or electron density of dPS, hPS, and hPI in the PS lamellae minus the average scattering length or electron density of dPS and hPI in the PI lamellae. As an intermediate case between model a and model d, one may consider the case where a part

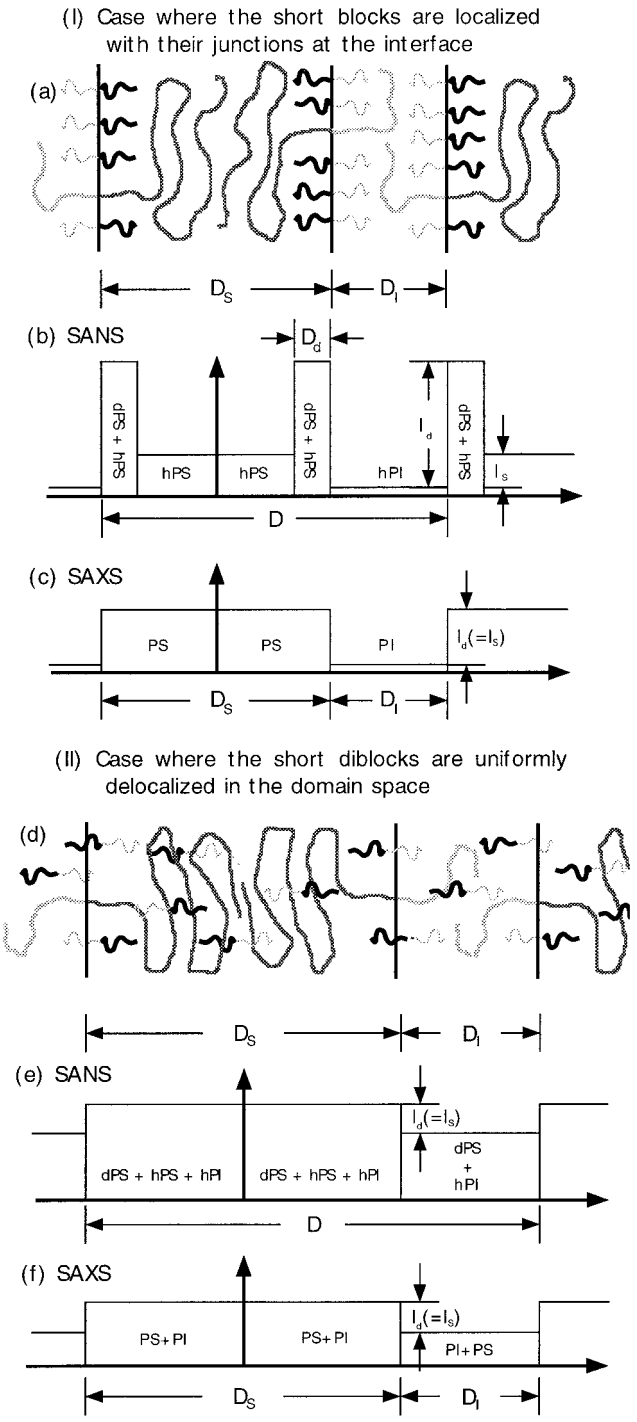

Figure 5. Model of blend of two diblock copolymers: (a) spatial distribution of two diblock chains, (b) neutron-scattering length, and (c) electron density for the case where the short diblock copolymer chains are segregated to the interface; (d) spatial distribution of two diblock chains, (e) neutron-scattering length, and (f) electron density for the case where the short diblock copolymer chains are dissolved uniformly into both phases of the microphase-separated structure.

of the short diblock with a fraction of $\Phi_{s,deloc}$ is delocalized uniformly into (1) the PS domain or (2) the PI domain or (3) both PS and PI domains. In such a case, l_d and l_s in Figure 5b are the corresponding average scattering lengths, as will be discussed in the Appendix, later.

The scattering intensity distribution with q at a particular azimuthal direction for partially oriented or randomly oriented systems, $J(q)$, is then described by

$$J(q) \propto q^{-2} f(q)^2 Z(q) \quad (2)$$

where the factor q^{-2} is the Lorentz factor for lamellar systems having an orientation distribution in 3D space with lateral dimensions much greater than their thickness.[35] $Z(q)$ is the paracrystal lattice factor which has maxima at $q = 2n\pi/D$ ($n = 1, 2, 3, ...$) and minima at q between those maxima and approaches unity with increasing q when the paracrystal distortion factors $g > 0$. However, since in this study we are primarily interested in the effect of the delocalization of the short block copolymers from the interface on the change of $f(q)$, below we ignore the effect of the paracrystalline distortion on the $J(q)$; namely, we assume a perfect crystal, $Z(q) = 1$ at $q = 2n\pi$/D ($n = 1, 2, 3, ...$) and $Z(q) = 0$ elsewhere. Thus, to obtain the scattered intensity for the first-order peak, with a domain spacing D, we would calculate $J(q = 2\pi/D)$. For the second order peak, we can readily calculate $J(q = 4\pi/D)$.

Note that we have ignored the effect of diffuse interfaces on SANS and SAXS. This is because we are primarily interested in the SANS profiles in the low-angle region for which we have high quality data. The diffuse interfaces mainly affect the scattering profile at large q values.[36,37] With this model, the height of the scattering peaks is a function of the volume fractions and scattering lengths of each region of the sample. Also, we have ignored the point that the grains of lamellae are small and not perfectly ordered. The measured peaks will be further weakened and broadened due to finite grain size, a lattice distortion of the lamellar stacks, etc.[35,36]

The most important feature of eq 1 is that the scattering amplitude from the form factor is the difference of two trigonometric functions. Therefore, for certain cases, we can expect to observe a zero scattering intensity $f(q)^2$ at the first-order peak of $Z(q)$. The diblock copolymers and blend concentrations used in this study were chosen to highlight this effect. To specify the scattering amplitude of the form factor, $f(q)$, we must identify the scattering length or electron density differences between each domain (l_d and l_s) and their sizes (D_d, D_S) as a function of $\Phi_{s,deloc}$. From the preparation of the blend sample, we know the fractions of long and short block copolymers, and we assume that the long diblock is completely and perfectly segregated under any condition. Then, given the fraction of the short diblocks which remain at the interface, $1 - \Phi_{s,deloc}$, the fraction of the short diblocks which are uniformly dissolved in the PS domain of the long diblock, $\Phi_{s,deloc}x_{s,deloc,PS}$, where $x_{s,deloc,PS}$ is a fraction of the delocalized short blocks which is dissolved in the PS phase, and the overall domain spacing, D, we can specify $f(q)$ by the calculation, the detail of which is given in the Appendix. Note that D is also a function of $\Phi_{s,deloc}$,but we do not know the exact relation between D and $\Phi_{s,deloc}$. Moreover, from eqs 1 and 2, we see that at $q = 2\pi/D$ or $4\pi/D$, $J(q)$ is just proportional to D,[4] then here we use the simplifying assumption that in any case D is constant at 31.4 nm.

To show the behavior of this equation, we will consider four extreme cases: (1) the short diblock copolymers are perfectly localized with their junctions at the interface; (2) a fraction of the short diblock copolymers leave from the interface and move to only the PS phase; (3) a fraction of the short diblock copolymers leave from the interface and move to only the PI phase; (4) a fraction of the short diblock copoly-

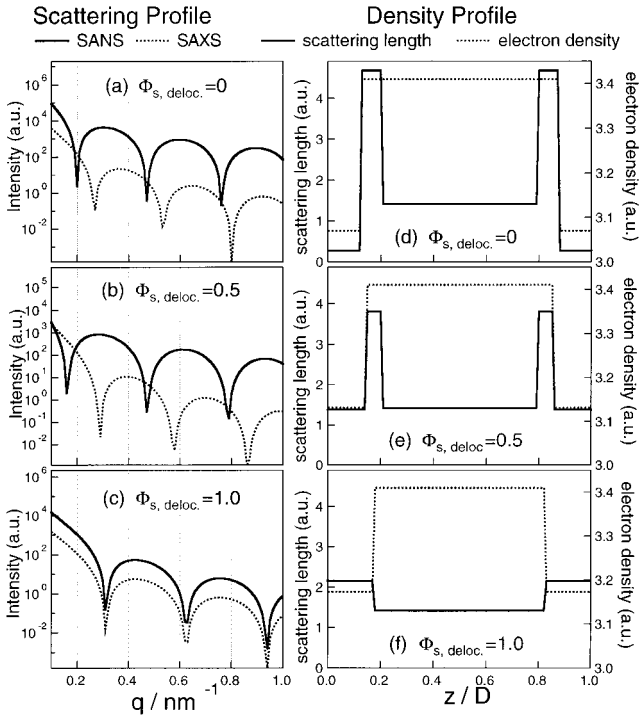

Figure 6. Results of model calculations for scattering profiles of SANS and SAXS (a−c) and corresponding density profiles (d−f) for the 80/20 blend at various $\Phi_{s,deloc}$, i.e., fraction of short diblock copolymers which are delocalized from the interface and moved to the PI phase. Key: (a and d) $\Phi_{s,deloc} = 0$; (b and e) $\Phi_{s,deloc} = 0.5$; (c and f) $\Phi_{s,deloc} = 1$. z is the coordinate normal to the interface.

mers leave from the interface and move to both PS and PI phases with the same ratio (i.e., 50% to PS phase and 50% to PI phase). The model calculates the scattering amplitudes as a function of the distribution of the short diblock copolymers, i.e., as a function of $\Phi_{s,deloc}$ and $x_{s,deloc,PS}$, which we cannot yet relate to a particular temperature.

To show the effect of the delocalization of the short diblock copolymer from the interface on the scattering profile clearly, in Figure 6 we depict some typical scattering length and electron density profiles of 80/20 blend and calculate the corresponding scattering profiles of $q^{-2}f(q)^2$ vs q, with changing $\Phi_{s,deloc}$. Parts a−c of Figure 6 show the calculated SAXS and SANS profiles (the form factor corrected for the Lorentz factor) of $q^{-2}f(q)^2$ vs q at $\Phi_{s,deloc} = 0$, 0.5, and 1.0, respectively. Parts d−f of Figure 6 show the scattering length and electron density profiles at $\Phi_{s,deloc} = 0$, 0.5, and 1.0 respectively, where the axes of abscissa are scaled with the total domain spacing, D. Note that for the calculation of Figure 6, we assume the extreme case (3) mentioned above; that is, all of the short diblock copolymers which leave the interface move to the PI phase. Figure 6 clearly shows that the calculated SANS profile, in particular the scattered intensity level, changes dramatically as the short diblock copolymer location changes, whereas the calculated SAXS profile changes only slightly. For example, in the SAXS profile the position of the first minimum increases gradually and monotonically with increasing $\Phi_{s,deloc}$, due to the slight decrease of the volume fraction of the PS phase. On the other hand, in the SANS profile the position of the first minimum changes more sensitively and complexly with the change in $\Phi_{s,deloc}$. This complicated behavior of the SANS profile is due to the large

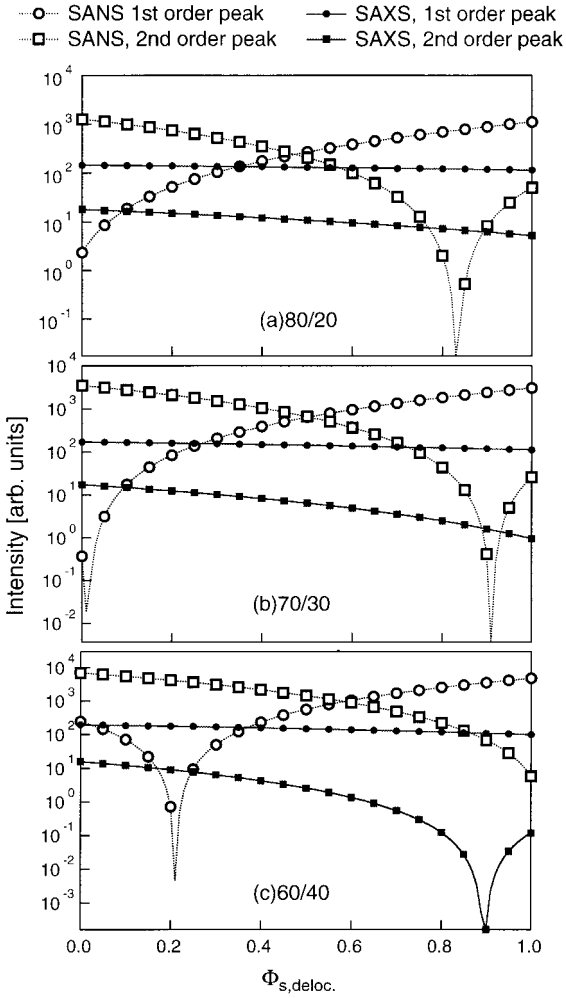

Figure 7. Results of model calculations for each blend for the case where the short diblock is uniformly dissolved into the PI microdomains. Predicted SANS (unfilled symbols, dashed lines) and SAXS intensities (filled symbols, solid lines) at the first-order peak (circles) and the second-order peak (squares) were plotted as a function of $\Phi_{s,deloc}$: (a) 80/20 blend; (b) 70/30 blend; (c) 60/40 blend.

scattering length difference between dPS and hPS and/or hPI. Hence, SANS is a much more sensitive method for testing whether the short diblock copolymer is moving from the interface into one particular microphase.

In Figure 7, we plot the calculated height of the first- and second-order SANS and SAXS peaks as a function of the fraction of the short diblock delocalized from the interface, $\Phi_{s,deloc}$. Here we further assume the delocalized short diblock copolymers are uniformly dissolved into the polyisoprene domain only. In this case scattering depends only on $\Phi_{s,deloc}$. In this way, going to the right along the abscissa corresponds to increasing temperature if $\Phi_{s,deloc}$ increases with temperature. In Figure 7, we note for all blends the small decreases in the first- and second-order SAXS peak intensities, which correspond to the changing volume fraction of each phase of the lamella. The exception is the second-order SAXS peak of the 60/40 blend which goes to zero when the volume fraction of each microphase reaches 0.5. This shows that with very careful SAXS measurements, it may be possible to observe the change in $\Phi_{s,deloc}$ with temperature. Careful measurements are required because the intensity change is small with $\Phi_{s,deloc}$. However, SAXS and SANS peak intensities will also change

with changes in grain size and degree of order inside the grain, making interpretation of the SAXS data alone difficult. It is expected that with decreasing temperature SAXS peak heights will increase not only due to the change in $\Phi_{s,deloc}$ but also due to improving order in the lamellar stacks. Since the latter gives the same effects as the former, that is, the short diblock migrating to the interface, one must separate the two effects. Such difficulty can be avoided by taking advantage of the SANS arising from the deuterium-labeling effect.

Figure 7 also shows that the SANS peak intensities change dramatically as the short diblock copolymer location changes. For example, in the case of the 80/20 and 70/30 mixtures, the first-order SANS peak intensity is very small when $\Phi_{s,deloc}$ is nearly zero; i.e., most of the short diblock copolymers are localized at the interface, and in the case of the 60/40 mixture, it plunges to zero when 20% of the short diblock copolymers migrate to the PI phase. Furthermore, the first-order scattering peak is weak compared to the second-order scattering peak for all three cases when $\Phi_{s,deloc} \leq$ ca. 0.5. These results are easily discerned as they are much more dramatic than the small changes in the SAXS peak scattering intensities. Furthermore, due to the nature of these changes, they cannot be confused with the effects of grain size and distortion in lamellar stacks[35−37] (paracrystalline lattice distortion[38]). For example, for the 80/20 and 70/30 blends, with increasing temperature, increasing lattice distortion in the lamellar stacks will lead to decreased peak heights. However, as $\Phi_{s,deloc}$ increases from a value of about 0.1 to a higher value such as 0.2, the first-order peak height will increase. Thus, an increase in peak height could clearly be identified as a change in location of the short diblock, since it is opposite to what is expected from the grain size and lattice distortion effects.

If we postulate that the short diblock segregates to the interface or $\Phi_{s,deloc}$ decreases with decreasing temperature, then we note that the trends shown in Figure 7 are matched by those observed in our scattering experiments, as shown in parts a and b of Figure 8, where we plot the first-order and second-order SANS peak heights, evaluated from Figure 4 as a function of temperature. That is, for some cases, the first-order scattering peak is very low or completely suppressed (i.e., has zero intensity) as observed in the 70/30 blend at all temperatures, and for the 60/40 blend at the temperatures below 140 °C. These correspond to the cases where $\Phi_{s,deloc} \cong 0.01$ for 70/30 (Figure 7b) and 0.21 for 60/40 (Figure 7c). Furthermore, the second-order peak should rise as the first-order peak falls with decreasing $\Phi_{s,deloc.}$ toward ca. 0.21 from a large value for the 60/40 blend as shown in Figure 7c, which matches the results observed in the 60/40 blend with decreasing temperature (Figure 8). As we lower temperature, we expect both peaks to rise from the SAXS experiments due to the increasing order in the sample and/or change in $\Phi_{s,deloc.}$. Finally, in the 80/20 blend, the first- and the second-order peak heights increase with decreasing temperature, which may be due to the fact that the peak heights increase anyway due to an increasing order with lowering temperature (i.e., increasing segregation power). Or, it could be due to the fact that for this blend composition, $\Phi_{s,deloc}$ is very insensitive to the change of temperature. Recall that the domain spacing behavior of the 80/20 blend was also similar to that of usual block copolymers.

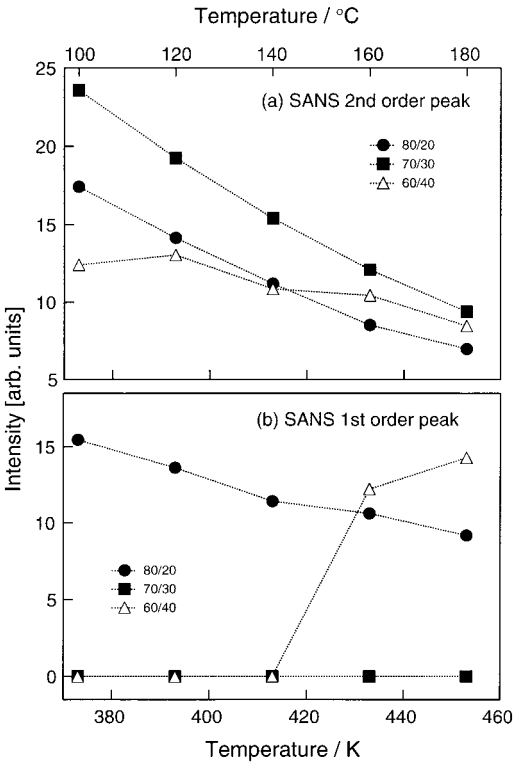

Figure 8. (a) Second-order and (b) first-order SANS peak intensities, evaluated from Figure 4, as a function of temperature. Key: (●) 80/20 blend; (■) 70/30 blend; (△) 60/40 blend.

In Figure 9, we have plotted the ratio, $R \equiv I_{m,1}/I_{m,2}$, of the first-order peak height, $I_{m,1}$, and the second-order peak height, $I_{m,2}$, which are evaluated from the calculated SANS profile such as shown in Figure 6a−c for the case where the short diblock copolymer moves to the PI microphase (solid line), the case where the short diblock copolymer moves to the PS microphase (dashed line), and the case where the short diblock copolymer moves to both PS and PI microphases with the same ratio(dash−dot line). We see in these plots that for the 70/30 blend it is possible to observe an R value of nearly zero when $\Phi_{s,deloc}$ is nearly zero; i.e., the short diblock copolymers are perfectly localized at the interface (Figure 9b), and for the 60/40 blend, an R value of nearly zero can be attained when 20% of the short diblock copolymers move to the PI microphase or 30% of short diblock copolymers move to both PS and PI microphase with the same ratio (Figure 9c).

We can now compare Figure 9 with Figure 10, which shows the experimental results of R evaluated again from Figure 4. We will consider the three extremes described above, but recognize that the sample is likely to be truly an intermediate case. Unfortunately, we cannot discern the exact case with these data.

For the case of the 80/20 blend, we see that the ratio is not zero but roughly unity at any temperature in Figure 10. This rules out the idea that we are observing about 8% of the short diblock being delocalized to the PS phase and also about 60% of the short diblock being delocalized to both PS and PI phase (Figure 9a). Furthermore, the experimental data show that with increasing temperature, the ratio is increasing slightly from 0.89 to 1.32 (Figure 10). The increasing ratio with increasing temperature rules out only the case where up to 60% of the short diblocks move to both PS and PI microphase with increasing temperature, and it does not

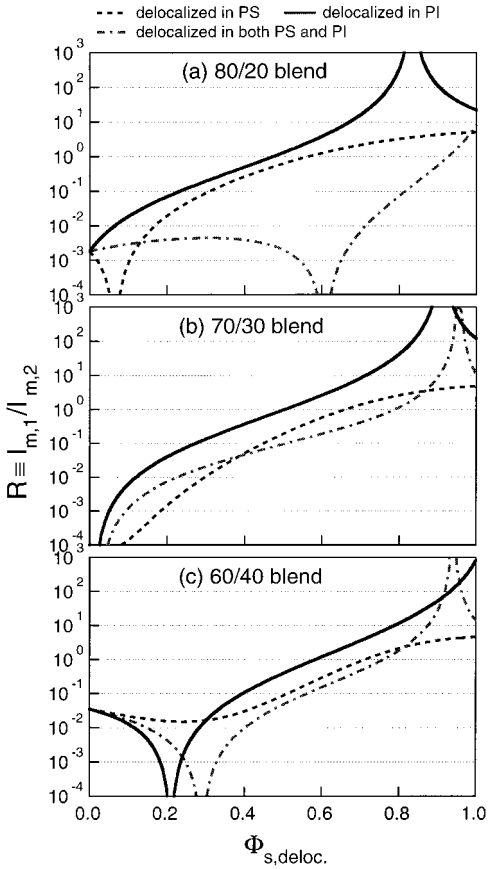

Figure 9. Results of model calculations for the case where the short diblock is uniformly delocalized in PS (dashed lines), PI (solid lines), and both PI and PS lamellae (dash−dot lines). The ratio of intensity of SANS first-order peak intensity over second-order peak intensity was plotted as a function of $\Phi_{s,deloc}$: (a) 80/20 blend; (b) 70/30 blend; (c) 60/40 blend.

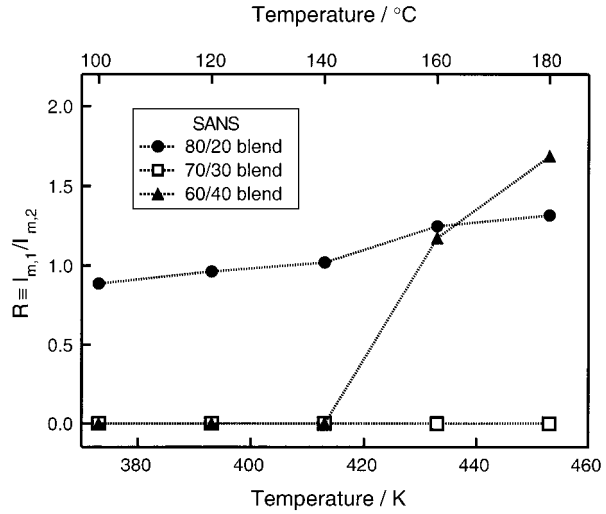

Figure 10. Ratio of SANS peak intensities as a function of temperature evaluated from Figure 4. Key: (●) 80/20 blend; (□) 70/30 blend; (▲) 60/40 blend.

give us any other information as to where and what amount of the short diblocks moves with increasing temperature. Note furthermore that the increasing ratio with increasing temperature is very common behavior in the PS−PI block copolymer system, because the distortion in the ordered lamellar stacks with increasing temperature leads to a decrease in the height of the second-order scattering peak compared to the first-order scattering peak, and an increase in the value of R. Thus, for this blend the experimental data is inconclusive.

For the case of the 70/30 blend, we observe that at all temperatures at which we measured, the value R is zero. That is, the first-order peak was not discerned over the temperature range measured. In Figure 9b, this case can correspond to that of the short diblock being considerably localized at the interface over the temperature range measured. Note, furthermore, that this interpretation is somewhat consistent with the SAXS data as shown in Figure 2b; that is, in Figure 2b we can clearly discern the second-order peak even at the highest temperature, 180 °C. This indicates that the order in the sample is still stable at 180 °C and indirectly suggests that the short diblock can still be at the interface.

Finally, for the 60/40 blend, the ratio is observed to be zero at lower temperatures and then to increase above zero at temperatures above 130 °C. This can correspond to the case where about 20% of the short diblock is dissolved in the PI domain at lower temperatures, and with increasing temperature more of the short diblock is dissolved into the PI domain. The data can also correspond to the case where about 30% of the short diblock copolymer is dissolved in both microdomains equally at lower temperatures, and with increasing temperature, the volume fraction delocalized from the interface is increasing.

The data are insufficient to clearly identify into which microphase the short diblock dissolves. However, the SANS data do match the model where the amount of short diblocks at the interface varies with temperature. The data from the 60/40 blends suggest the short diblock is not selectively dissolved into the PS microphase due to the presence of zero values for R. Since the PI block of the long diblock copolymer is of much lower molecular weight than the PS block of the copolymer, we expect that the short symmetric diblock is more soluble in the PI block, and the SANS is consistent with our expectations. However, SANS does not rule out the case where the diblock is dissolved in both equally.

We emphasize that all of these measurements were made at temperatures above the T_g of the polystyrene (over 100 °C).

Thus, we can see that the simple model of the scattering behavior discussed above that includes the short diblock at the interface can describe the unusual neutron scattering observed in these samples.

V. Concluding Comments

We have used evidence from SAXS and SANS to support the idea that the short diblock copolymer is located with their junctions at the interface in a diblock copolymer/diblock copolymer blend system and that with an increase in temperature, the short diblock tends to delocalize away from the interface. The effect of temperature on the domain spacing as measured by SAXS suggests that the short diblock leaves the interface with increasing temperature leading to unusual temperature dependence of the domain spacing. Furthermore, the unusual SANS results strongly support this idea. The SANS patterns are very unusual in that the first-order scattering peak is very weak or completely suppressed. However, the results can be explained by the presence of the short diblock copolymer at the interface. The temperature-dependent SANS results show the short diblock being delocalized from the interface with in-

creasing temperature. In the future, it would be useful to examine the location of the short diblock in more detail.

Appendix

Calculation of the Scattering Contrast and Size of Each Domain as a Function of the Delocalized Short Diblock Copolymer Fraction, $\Phi_{s,deloc}$. Below we describe the procedures employed in this study to obtain the scattering contrasts and sizes of dPS-, hPS-, and hPI-rich regions which are necessary for the calculation of the scattering amplitude, $f(q)$, given in eq 1. The parameters l_d and l_s in eq 1 are expressed as

$$l_d = \rho_{dPS} - \rho_{hPI} \tag{A1}$$

$$l_s = \rho_{hPS} - \rho_{hPI} \tag{A2}$$

where ρ_i (i = dPS, hPS, or hPI) is the scattering contrast, that is, the scattering length density for SANS and electron density for SAXS, of the i-rich region. Note that the dPS-rich region contains both dPS and hPS, and hence ρ_{dPS} reflects the scattering contrast of dPS and hPS. Also, the domain widths of i-rich region, D_i (i = dPS, hPS, or hPI), fulfill the expression

$$D = D_{hPS} + 2D_{dPS} + D_{hPI} \tag{A3}$$

where D is the domain spacing. From eq A3, we discern that the parameter D_S and D_d in eq 1 correspond to $D_{hPS} + 2D_{dPS}$ and D_{dPS} in eq A3, respectively.

The two diblock copolymers which compose the mixture, i.e., the long and asymmetric hPS-hPI coplymer, SI-56-12, and the short and symmetric dPS-hPI copolymer, dSI-5-4, are hereafter designated as α and β, respectively, and then the volume fractions of each region, $V_i \equiv D_i/D$ (i = dPS, hPS, or hPI) are expressed as

$$V_i = \sum_j V_{i,j} \text{ (i, j = dPS, hPS, or hPI)} \tag{A4}$$

where $V_{i,j}$ denotes the volume fraction of the j-th block (j = dPS, hPS, or hPI) in the i-th region.

$$V_{hPI,hPI} = v_\alpha(1 - f_\alpha) + v_\beta(1 - \Phi_{s,deloc})(1 - f_\beta) + v_\beta\Phi_{s,deloc}(1 - x_{s,deloc.,PS})(1 - f_\beta) \tag{A5}$$

$$V_{hPI,hPS} = 0 \tag{A6}$$

$$V_{hPI,dPS} = v_\beta\Phi_{s,deloc}(1 - x_{s,deloc,PS})f_\beta \tag{A7}$$

$$V_{dPS,dPS} = v_\beta(1 - \Phi_{s,deloc})f_\beta\left[1 + \frac{n_\alpha}{n_\beta(1 - \Phi_{s,deloc})}\frac{v_\beta\Phi_{s,deloc}x_{s,deloc,PS}f_\beta}{(v_\alpha f_\alpha + v_\beta\Phi_{s,deloc}x_{s,deloc,PS})}\right] \tag{A8}$$

$$V_{dPS,hPS} = v_\beta(1 - \Phi_{s,deloc})f_\beta\frac{n_\alpha}{n_\beta(1 - \Phi_{s,deloc})}\frac{v_\alpha f_\alpha}{(v_\alpha f_\alpha + v_\beta\Phi_{s,deloc}x_{s,deloc,PS})} \tag{A9}$$

$$V_{dPS,hPI} = v_\beta(1 - \Phi_{s,deloc})f_\beta\frac{n_\alpha}{n_\beta(1 - \Phi_{s,deloc})}\frac{v_\beta\Phi_{s,deloc}x_{s,deloc,PS}(1 - f_\beta)}{(v_\alpha f_\alpha + v_\beta\Phi_{s,deloc}x_{s,deloc,PS})} \tag{A10}$$

$$V_{hPS,hPS} = v_\alpha f_\alpha\left[1 - \frac{n_\alpha v_\beta f_\beta}{n_\beta(v_\alpha f_\alpha + v_\beta\Phi_{s,deloc}x_{s,deloc,PS})}\right] \tag{A11}$$

$$V_{hPS,dPS} = v_\beta\Phi_{s,deloc}x_{s,deloc,PS}f_\beta\left[1 - \frac{n_\alpha v_\beta f_\beta}{n_\beta(v_\alpha f_\alpha + v_\beta\Phi_{s,deloc}x_{s,deloc,PS})}\right] \tag{A12}$$

$$V_{hPS,hPI} = v_\beta\Phi_{s,deloc}x_{s,deloc,PS}(1 - f_\beta)\left[1 - \frac{n_\alpha v_\beta f_\beta}{n_\beta(v_\alpha f_\alpha + v_\beta\Phi_{s,deloc}x_{s,deloc,PS})}\right] \tag{A13}$$

Here v_i (i = α or β) is the volume fraction of the i-th copolymer in the mixture with $v_\alpha + v_\beta = 1$; f_i (i = α or β) is the volume fraction of polystyrene block in the i-th copolymer, and the value of which is described in the Experimental Section; n_i (i = α or β) is the mole fraction of i-th copolymer in the mixture with $n_\alpha + n_\beta = 1$; $\Phi_{s,deloc}$ and $x_{s,deloc,PS}$ are the same as defined in the Discussion.

Finally, the scattering contrasts of each region, ρ_i (i = dPS,hPS, or hPI), are expressed using eqs A4−A13 and

$$\rho_i = \frac{1}{V_i}\sum_j \rho_{j0}V_{i,j} \text{ (i, j = dPS, hPS, or hPI)} \tag{A14}$$

where ρ_{j0} (j = dPS, hPS, or hPI) is the scattering contrast of pure j-th monomer and we use the scattering length densities of $\rho_{dPS,0} = 6.49 \times 10^{10}$, $\rho_{hPS,0} = 1.42 \times 10^{10}$, and $\rho_{hPI,0} = 2.69 \times 10^9$ (cm/cm^3) for SANS and the electron densities of $\rho_{dPS,0} = 3.41 \times 10^{23}$, $\rho_{hPS,0} = 3.41 \times 10^{23}$, and $\rho_{hPI,0} = 3.07 \times 10^{23}$ (e/cm^3) for SAXS, respectively.

Acknowledgment. We would like to thank Dr. François Court for useful discussions. J.B. would like to thank JSPS for support of this research.

References and Notes

(1) Hashimoto, T. In *Thermoplastic Elastomers, A Comprehensive Review*; Legge, N. R., Holden, G., Schroeder, H. E., Eds.; Hanser: Munich, Germany, 1996; p 429. Hasegawa, H.; Hashimoto, T. In *Comprehensive Polymer Science, Second Supplement*; Aggarwal, S. L.' Russo, S. Volume Eds.; Pergamon: New York, 1996; p 497.
(2) Bates, F. S.; Fredrickson, G. H. *Annu. Rev. Phys. Chem.* **1990**, *41*, 525.
(3) Hadziioannou, G.; Skoulios, A. *Macromolecules* **1982**, *15*, 267.
(4) Hashimoto, T. *Macromolecules* **1982**, *15*, 1548.
(5) Hashimoto, T.; Yamasaki, K.; Koizumi, S.; Hasegawa, H. *Macromolecules* **1993**, *26*, 2895.
(6) Hashimoto, T.; Koizumi, S.; Hasegawa, H. *Macromolecules* **1994**, *27*, 1562.
(7) Koizumi, S.; Hasegawa, H.; Hashimoto, T. *Macromolecules* **1994**, *27*, 4371.
(8) Court, F. These de Doctorat de l'Université Pierre et Marie Curie, 1996.
(9) Spontak, R.; J.; Fung, J.; C.; Braunfeld, M. B.; Sedat, J. W.; Agard, D. A.; Kane, L.; Smith, S. D.; Satkowski, M. M.;

Ashraf, A.; Hajduk, D. A.; Gruner, S. M. *Macromolecules* **1996**, *29*, 4494.
(10) Hashimoto, T.; Tanaka, H.; Hasegawa, H. *Macromolecules* **1990**, *23*, 4378.
(11) Shi, A.-C.; Noolandi, J. *Macromolecules* **1994**, *27*, 2936.
(12) Shi, A.-C.; Noolandi, J. *Macromolecules* **1995**, *28*, 3103.
(13) Matsen, M. W.; Bates, F. S. *Macromolecules* **1995**, *28*, 7298.
(14) Lin, E. K.; Gast, A. P.; Shi, A.-C.; Noolandi, J.; Smith, S. D. *Macromolecules* **1996**, *29*, 5920.
(15) Sakurai, S.; Umeda, H.; Yoshida, A.; Nomura, S. *Macromolecules* **1997**, *30*, 7614.
(16) Hasegawa, H.; Hashimoto, T.; Kawai, H.; Lodge, T. P.; Amis, E. J.; Glinka, C. J.; Han, C. C. *Macromolecules* **1985**, *18*, 67.
(17) Hasegawa, H.; Tanaka, H.; Hashimoto, T. *Macromolecules* **1987**, *20*, 2120.
(18) Matsushita, Y.; Mori, K.; Mogi, Y.; Saguchi, R.; Noda, I.; Nagasawa, M.; Chung, T.; Glinka, C. J.; Han, C. C. *Macromolecules* **1990**, *23*, 4317.
(19) Matsushita, Y.; Mori, K.; Saguchi, R.; Noda, I.; Nagasawa, M.; Chang, T.; Glinka, C. J.; Han, C.; C. *Macromolecules* **1990**, *23*, 4387.
(20) Koizumi, S.; Hashimoto, T. *Physica B* **1995**, *213&214*, 703.
(21) Hasegawa, H.; Tanaka, T.; Hashimoto, T.; Han, C. C. *J. Appl. Crystallogr.* **1991**, *24*, 672.
(22) Mayes, A. M.; Russell, T. P.; Satija, S. K.; Majkrzak, C. F. *Macromolecules* **1992**, *25*, 6523.
(23) Matsushita, Y.; Torikai, N.; Mogi, Y.; Noda, I.; Han, C. C. *Macromolecules* **1993**, *26*, 6346.
(24) Koizumi, S.; Hasegawa, H.; Hashimoto, T. *Macromolecules* **1994**, *27*, 7893.
(25) Mayes, A. M.; Russell, T. P.; Deline, V. R.; Satija, S. K.; Majkrzak, C. F. *Macromolecules* **1994**, *27*, 7447.
(26) Winey, K. I.; Gobran, D. A.; Xu, Z.; Fetters, L. J.; Thomas, E. L. *Macromolecules* **1994**, *27*, 2392.
(27) Hashimoto, T.; Suehiro, S.; Shibayama, M.; Saijo, K.; Kawai, H. *Polymer Journal* **1981**, *13*, 501.
(28) Suehiro, S.; Saijo, K.; Ohta, Y.; Hashimoto, T. *Anal. Chim. Acta* **1986**, *189*, 41.
(29) Fujimura, M.; Hashimoto, T.; Kawai, H. *Mem. Fac. Eng., Kyoto Univ.* **1981**, *43* (2), 224.
(30) Hasegawa, H.; Tanaka, H.; Yamasaki, K.; Hashimoto, T. *Macromolecules* **1987**, *20*, 1651.
(31) Mori, K.; Hasegawa, H.; Hashimoto, T. *Polym. J.* **1985**, *17*, 799.
(32) Sakamoto, N.; Hashimoto, T. *Macromolecules* **1995**, *28*, 6825.
(33) Hashimoto, T.; Shibayama, M.; Kawai, H. *Macromolecules* **1983**, *16*, 1093.
(34) The readers might notice an excess scattering at the q region of 0.1 $nm^{-1} \leq q \leq 0.15$ nm^{-1} smaller than the q region where the first-order SANS peak exists. At this stage we are not sure whether this reflects an artifact arising from the edge of the beam stopper used in the SANS experiments or true scattering. This excess scattering is not strong and is not sensitive to the temperature change. Moreover, this excess scattering has no clear tendency to increase or decrease with decreasing temperature; i.e., the intensity I changes with temperatures T as follows: I at $T = 120$ °C > I at $T = 140$ °C > I at $T = 100$ °C > I at $T = 160$ °C > I at $T = 180$ °C. Therefore, we hereafter did not take into consideration this excess scattering.
(35) Shibayama, M.; Hashimoto, T. *Macromolecules* **1986**, *19*, 740.
(36) Hashimoto, T.; Nagatoshi, K.; Todo, A.; Hasegawa, H.; Kawai, H. *Macromolecules* **1974**, *7*, 364.
(37) Hashimoto, T.; Fujimura, M.; Kawai, H. *Macromolecules* **1980**, *13*, 1660.
(38) Hosemann, R.; Bagachi, S. N. *Direct Analysis of Diffraction by Matter*; North-Holland: Amsterdam, 1962.

MA990534O